

SLAC-PUB-8238  
October 1999

# Indirect Collider Tests for Large Extra Dimensions<sup>1</sup>

**Thomas G Rizzo**<sup>2</sup>

Stanford Linear Accelerator Center, Stanford CA 94309, USA

**Abstract.** We review the capability of colliders to detect the virtual exchange of Kaluza-Klein towers of gravitons within the low scale quantum gravity scenario of Arkani-Hamed, Dimopoulos and Dvali.

## 1. Introduction

Arkani-Hamed, Dimopoulos and Dvali(ADD) recently proposed a interesting low scale quantum gravity scenario which offers a new slant on the hierarchy problem[1]. In its simplest form, gravity is allowed to live in  $n$  ‘large’ extra dimensions, *i.e.*, ‘the bulk’, while the Standard Model(SM) fields lie on a 3-D surface or brane, ‘the wall’. Gravity then becomes strong in the full  $4 + n$ -dimensional space at a scale  $M_s \sim$  a few TeV which is far below the conventional Planck scale,  $M_{pl} \sim 10^{19}$  GeV. The scales  $M_s$  and  $M_{pl}$  are simply related via Gauss’ Law:

$$M_{pl}^2 = V_n M_s^{n+2}, \quad (1)$$

<sup>1</sup> To appear in the *Proceedings of Beyond the Desert99: Accelerator, Non-Accelerator and Space Approaches*, Castle Ringberg, Tegernsee, Germany, June 6-12 1999

<sup>2</sup> E-mail: [rizzo@slacvx.slac.stanford.edu](mailto:rizzo@slacvx.slac.stanford.edu). Work supported by the Department of Energy, Contract DE-AC03-76SF00515

with  $V_n$  being the volume of the compactified extra dimensions. For  $n$  extra dimensions of the same size, the simplest possibility, termed a symmetric compactification,  $V_n \sim R^n$  and one finds that  $R \sim 10^{30/n-19}$  meters assuming  $M_s \sim 1$  TeV. Note that for separations between two masses less than  $R$  the gravitational force law becomes  $1/r^{2+n}$ . For  $n = 1$ ,  $R \sim 10^{11}$  meters and is thus obviously excluded, but, for  $n = 2$  one obtains  $R \sim 0.1$  mm, which is at the edge of the sensitivity for existing experiments[2]. One can imagine more general scenarios, termed asymmetric compactifications, where, *e.g.*, there are  $p$  ‘small’ dimensions that have sizes of  $\sim 1/TeV$  with the effective number of ‘large’ extra dimensions being  $n_{eff} = n - p$ , where now  $n = 6$  or  $7$  as suggested by string theory[3]. Astrophysics[4] requires that  $M_s > 110$  TeV for  $n = 2$  but only  $\geq$  a few TeV for  $n > 2$ .

The ADD scenario is based on the assumption that the metric tensor factorizes, *i.e.*, that the usual 4-D components are independent of the co-ordinates of the other dimensions. Giving up this assumption can lead to a number of other interesting scenarios with completely different phenomenology[5].

The Feynman rules[6] for the ADD scenario are obtained by considering a linearized theory of gravity in the bulk, decomposing it into the more familiar 4-D states and recalling the existence of Kaluza-Klein towers for each of the conventionally massless fields. The entire set of fields in the K-K tower couples in an identical fashion to the particles of the SM. By considering the forms of the  $4+n$  symmetric, conserved stress-energy tensor for the various SM fields and by remembering that such fields live only on the wall one may derive all of the necessary couplings. An important result of these considerations is that only the massive spin-2 K-K towers (which couple to the 4-D conserved, symmetric stress-energy tensor,  $T^{\mu\nu}$ ) and spin-0 K-K towers (which couple proportional to the trace of  $T^{\mu\nu}$ ) are of phenomenological relevance as all the spin-1 fields can be shown to decouple from the particles of the SM. For processes that involve massless fields at at least one vertex, as will be the case below, the contributions of the spin-0 fields can also be ignored.

Outside of table top experiments and astrophysics, the two ways of probing this scenario are via the emission of KK towers of gravitons in scattering processes or through the exchange of KK graviton towers between SM fields[6, 7]. In the case of emission, one uses the Feynman rules to calculate the cross section for the production of a graviton of fixed mass and then sums over the full tower of states. If the mass splittings among the gravitons are small in comparison to the typical energy scale of the process of interest we can replace the summation by an integral weighted by the  $n$ -D density of states and which is cut off by the specific process kinematics. Due to the huge number of KK states which are integrated over the typical  $M_{pl}$  suppression one expects from gravity vanishes and

is replaced by suppression due to simple powers of  $E/M_s$ , with  $E$  being the typical energy scale in the relevant interaction. Perhaps the simplest process of this kind is  $e^+e^- \rightarrow G_n\gamma$ , with  $G_n$  representing the tower of gravitons that appear as missing energy in a detector. Fig.1 shows the typical signal cross section and background for this process at LEP II for different numbers of extra dimensions with  $M_s = 1$  TeV which is close to the present experimental bound[8] for  $n = 2$ .

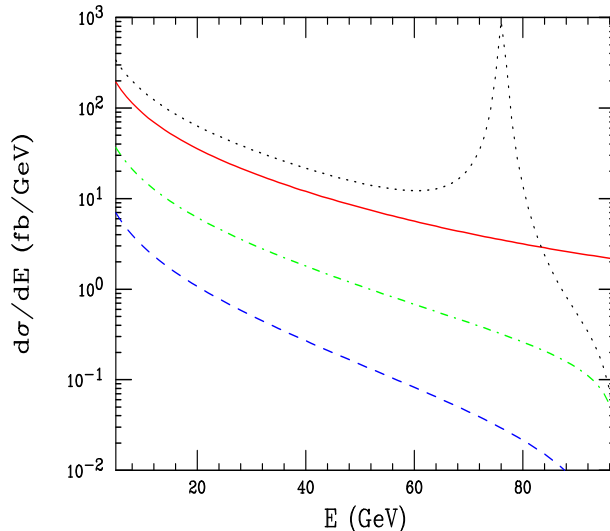


**Figure 1.** Cross section with  $\sqrt{s} = 195$  GeV for  $e^+e^- \rightarrow G_n\gamma$  as a function of the photon energy assuming  $M_s = 1$  TeV with 2(3,4) extra dimensions corresponding to the solid(dash-dotted, dashed) curve. The dotted curve is the SM background.

## 2. Graviton Exchange

The virtual exchange of graviton towers either leads to modifications in SM cross sections and asymmetries or to new processes not allowed in the SM at the tree level. In the case of exchange the amplitude is proportional to the sum over the propagators of the entire KK tower which naively diverges when  $n > 1$  even when transformed to an integral over the density of states. This integral can either be regulated by a brute force cut-off, by the tension of the 3-brane[9], or through the finite extent of the SM fermion wave functions in the additional dimensions[10]. The differential cross sections then become relatively  $n$  insensitive functions of the effective cut-off scale,

traditionally taken as  $M_s$ , and the overall sign of the dimension-8 operator induced by the KK tower,  $\lambda$ . Thus effectively, we essentially have the replacement

$$\frac{i^2}{8\overline{M}_{Pl}^2} \sum_{n=1}^{\infty} \frac{1}{s - m_n^2} \rightarrow \frac{\lambda}{M_s^4}. \quad (2)$$

where  $\overline{M}_{Pl}$  is the reduced Planck scale. Note that this replacement is *universal* in that it is independent of the choice of particles in the initial or final state. Similar substitutions also take place in the  $t$ - and  $u$ -channels allowing for the straightforward calculation of a large number of cross sections for different processes. A characteristic feature in all cases is the rapid growth with energy of the graviton contribution to the amplitude; relative to the pure SM, interference terms go as  $\sim s^2/M_s^4$  whereas the pure gravity terms behave as  $\sim s^4/M_s^8$ . For  $s$  significantly larger than  $M_s^2$  tree level unitarity is violated but, long before that, we would expect other operators, higher order quantum gravity and stringy effects to become important providing some sort of a natural cut off. As one can imagine, there are a huge number of processes that one can now examine for KK exchange sensitivity and we can only review some of them here. We refer the interested reader to the original literature[7].

### 3. Lepton Colliders

Due to the spin-2 nature of the gravitons in the tower, angular distributions (and polarization asymmetries) become particularly sensitive probes of this scenario. For example, the differential cross section for the process  $e^+e^- \rightarrow f\bar{f}$  now contains both cubic as well as quartic terms in  $\cos\theta$  and is shown in Fig.2 for  $f = b$  at LEP II energies. In all such processes the interference between the SM and graviton KK tower exchanges is found to vanish when all angles are integrated over thus emphasizing the importance of examining differential distributions when trying to constrain  $M_s$ .

Hewett[6] performed a combined fit of the angular distributions of all kinematically accessible  $f\bar{f}$  final states, as well as the polarization of the  $\tau$ , to obtain a potential search reach for LEP through these channels of  $M_s \simeq 1$  TeV for either sign of  $\lambda$ . She also demonstrated that  $e^+e^-$  colliders could distinguish the particular deviations induced by these spin-2 exchanges from those due to lower spins, such as a  $Z'$  or  $\tilde{\nu}$  in R-parity violating models[11], or from exchanges in other channels, such as leptoquarks[12], almost up to the search reach. Such an analysis can be extended to the case of a 500 GeV or 1 TeV linear collider with the results as shown in Fig.3. Here not only are the differential cross sections employed but also the angular dependent polarization asymmetries, shown in Fig.2 for the case of the  $b$  quark, since the initial electron beam can now be polarized.

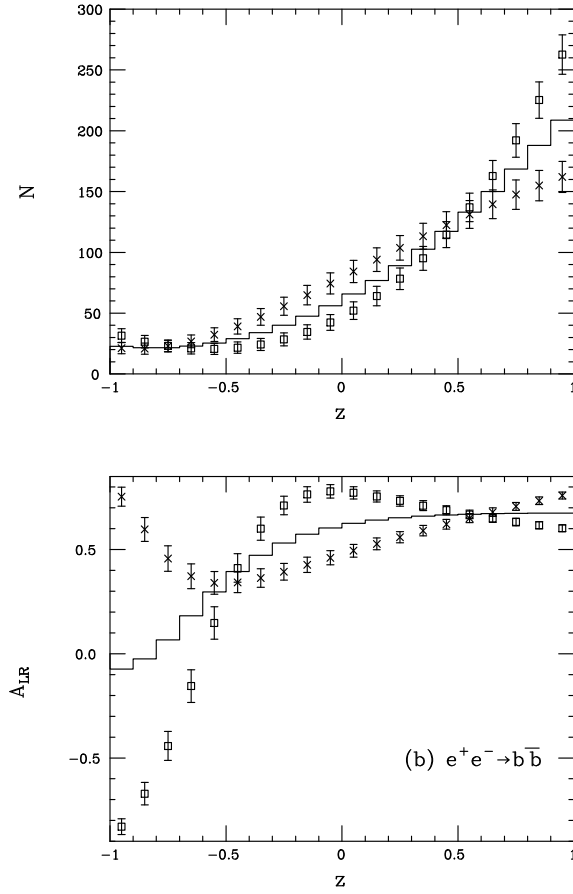


**Figure 2.** Distortions(top) in the bin integrated SM cross section(histogram) for  $e^+e^- \rightarrow b\bar{b}$  at  $\sqrt{s} = 200$  GeV with a luminosity of  $1 \text{ fb}^{-1}$  assuming  $M_s = 0.6$  TeV. The two sets of ‘data’ correspond to  $\lambda = \pm 1$ . The corresponding distortions in the  $b$  Left-Right Asymmetry at a 500 GeV linear collider are shown in the bottom panel assuming a luminosity of  $75 \text{ fb}^{-1}$ .

We see that the reach from such a combined channel analysis of this type is of order  $M_s \sim 6 - 7\sqrt{s}$ .

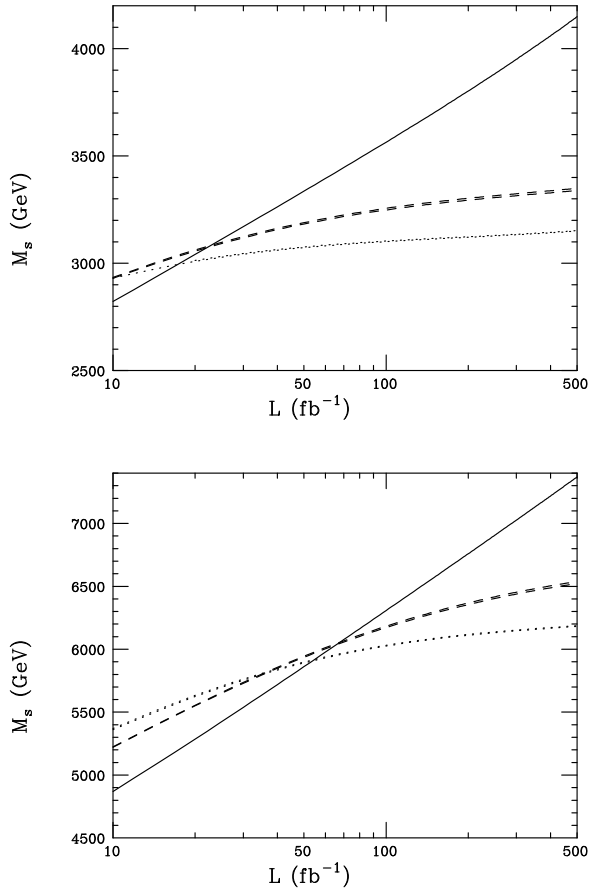


**Figure 3.** Search reaches for  $M_s$  at a 500 GeV(top) and 1000 GeV(bottom)  $e^+e^-/e^-e^-$  collider as a function of the integrated luminosity for Bhabha(dashed) and Moller(dotted) scattering for either sign of the parameter  $\lambda$  in comparison to the ‘usual’ search employing the combined channel  $e^+e^- \rightarrow f\bar{f}$ (solid) fit as described in the text.

$e^+e^-$  annihilation into gauge boson pairs also can provide reasonable sensitivity to  $M_s$  as shown in Figs.4 and 5 for  $W^+W^-$  and  $ZZ$  production at LEP II, respectively. We note that unlike what happens in many other new physics scenarios, the  $W^+W^-$  total cross section can actually be *de-*

created through the exchange of KK towers of gravitons. While the KK towers do not lead to any appreciable modification of the  $ZZ$  angular distribution, they modify the  $W^+W^-$  distribution in the backwards direction due to the dominance of the SM  $t$ -channel  $\nu$  exchange graph. The KK tower exchange is found to lead to essentially insignificant modifications in the helicity fractions of the final state gauge bosons at LEP II energies although the effects are somewhat larger at higher energy colliders[7]. The differential cross section modifications in the case of the  $\gamma\gamma$  final state are similar to those of  $ZZ$ .

As mentioned earlier, graviton exchange can lead to new processes which are forbidden at the tree level in the SM. An excellent example of this is provided by the process  $e^+e^- \rightarrow 2h$  where  $h$  is a Higgs boson; in the SM or MSSM this process can only occur at the one-loop level. The angular distribution induced from the tree level graviton exchange and that arising from loops are quite distinct since the graviton exchange graph leads to a distribution quartic in  $\cos\theta$ . The cross section is reasonably large with measurable rates possible at future linear colliders for  $M_s \sim 1$  TeV but are found to decrease rapidly as  $M_s$  is increased, *i.e.*,  $\sigma \sim s^3/M_s^8$  as shown in Fig.6.

#### 4. Hadron Colliders

Hadron colliders such as the Tevatron and LHC offer many distinctive probes for the exchange of KK towers of gravitons. Here we will limit our discussion to the Drell-Yan process and top quark pair production.

An interesting feature of the ADD scenario in the case of Drell-Yan channel is the contribution of  $gg$  initial state to the charged dilepton pair production, *i.e.*,  $gg, q\bar{q} \rightarrow G_n \rightarrow \ell^+\ell^-$ . This additional amplitude helps to increase the  $M_s$  reach for this process, particularly at the LHC where the  $gg$  luminosities are so large. As in the case of  $e^+e^- \rightarrow f\bar{f}$ , the KK exchange modifies both the cross section as well as the angular distribution as probed by the Forward-Backward asymmetry,  $A_{FB}$ . In the case of the total cross section as the invariant pair mass of the leptons approaches  $M_s$  there is a substantial rise in the cross section, for either sign of  $\lambda$ , appearing in the form of a shoulder as is typical of contact interaction signatures. Similarly as the scale  $M_s$  is approached from below the magnitude of  $A_{FB}$  is seen to decrease towards zero. This is easily understood since the graviton KK tower couplings are  $C$  and  $P$  conserving thus leading to a angular distribution for leptons which involve only even powers of  $\cos\theta$  and a null asymmetry. Fig.7 shows how these deviations would appear at hadron colliders. Hewett[6] has estimated the  $M_s$  search reach for the Drell-Yan channel at both the Tevatron and LHC by performing a fit to both the bin

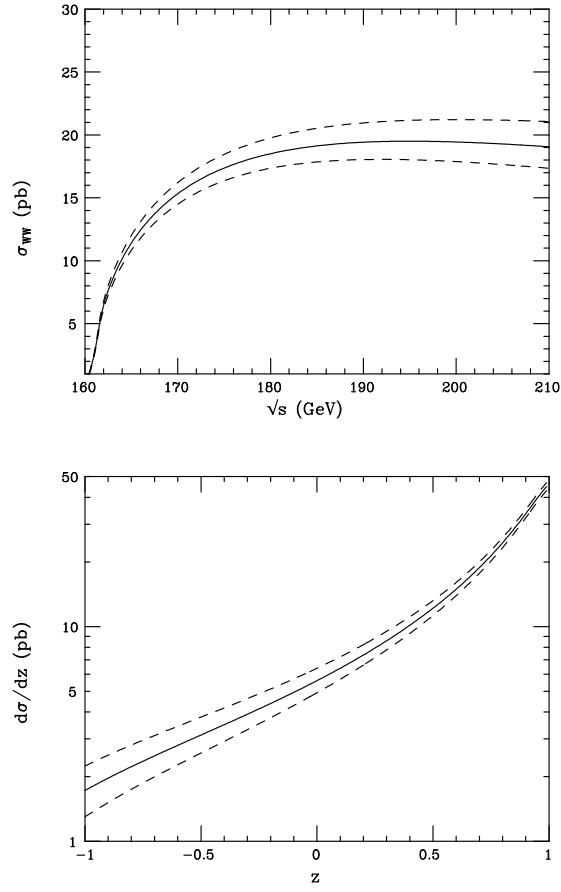


**Figure 4.** Total cross section and angular distribution for  $W^+W^-$  production at LEP II energies for the case of the SM (solid) or the ADD model with  $M_s = 0.6$  TeV and  $\lambda = \pm 1$  (dashed). The angular distribution in the lower panel is for  $\sqrt{s} = 200$  GeV. Note  $z = \cos\theta$ .



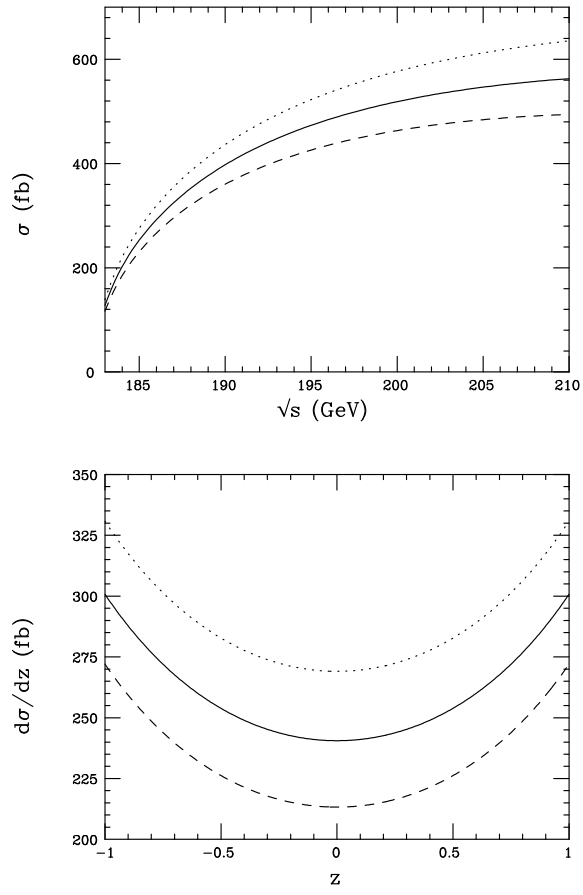


**Figure 5.** Same as in the previous figure but now for the  $ZZ$  final state.

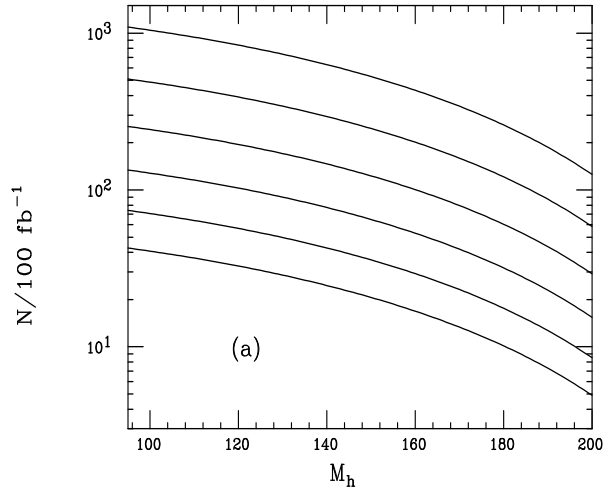


**Figure 6.** Tree level production rate for Higgs boson pairs due to graviton tower exchange at a 500 GeV  $e^+e^-$  collider as a function of the Higgs mass scaled to an integrated luminosity of  $100 \text{ fb}^{-1}$ . From top to bottom the curves correspond to the choice  $M_s = 1 \text{ TeV}$  increasing in steps of 0.1 TeV.

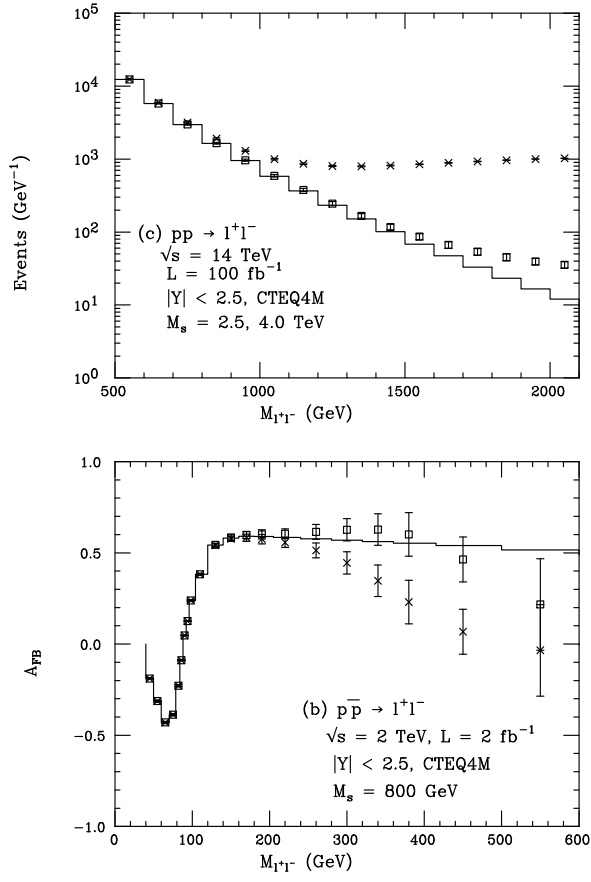


**Figure 7.** Drell-Yan cross section at the LHC in the SM(histogram) as well as for  $M_s=2.5$  or 4 TeV.  $A_{FB}$  at the Tevatron with  $M_s=0.8$  TeV for either sign of  $\lambda$ .

integrated total cross section and  $A_{FB}$  and obtained the results shown in Fig.8. In particular we see that the LHC reach is  $\simeq 5.3$  TeV, somewhat less than that obtainable at a 1 TeV linear collider.

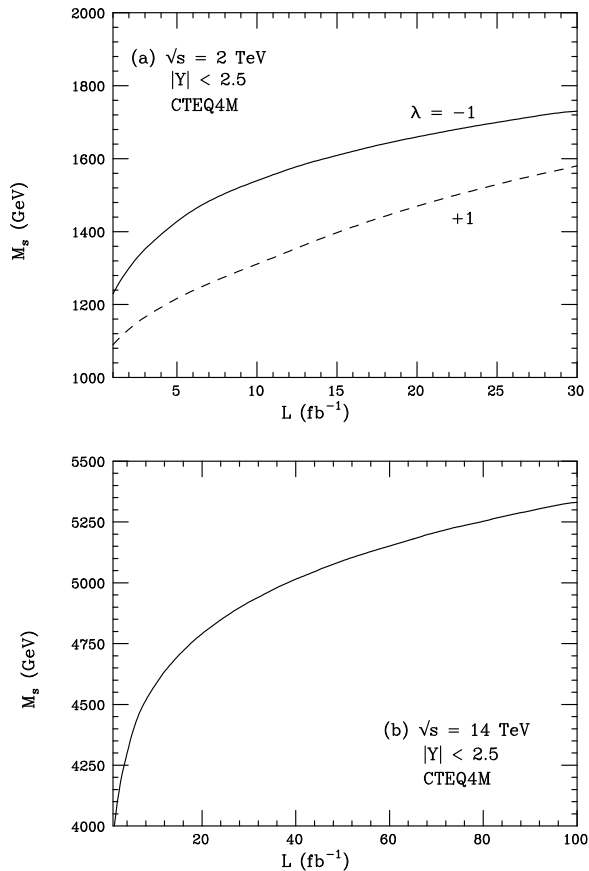


**Figure 8.**  $M_s$  reaches at the Tevatron and LHC from Drell-Yan.

In the case of top pair production it has been shown that the deviation in the cross section due to graviton tower exchanges,  $gg, q\bar{q} \rightarrow G_n \rightarrow t\bar{t}$ , is not the best probe for large values of  $M_s$ . (The respective deviations in the total  $t\bar{t}$  cross sections at the Tevatron and LHC due to KK gravitons are shown in Figs.9 and 10.) Thus in order to gain in sensitivity we must look at the various distributions. It[7] has also been shown that neither the rapidity nor the top quark angular distributions are particularly sensitive to these new contributions. However, the top quark  $p_t$  and top pair invariant

mass distributions do show substantial sensitivity to finite  $M_s$  as is also shown in Figs. 9 and 10. Performing a simultaneous fit to both the  $p_t$  and  $M_{t\bar{t}}$  distributions leads to a reach of 1.2(6) TeV at the Run II Tevatron with an integrated luminosity of  $2\text{ fb}^{-1}$  (LHC with an integrated luminosity of  $100\text{ fb}^{-1}$ ). These values are quite comparable to but somewhat better than those obtained through the analysis of the Drell-Yan channel.

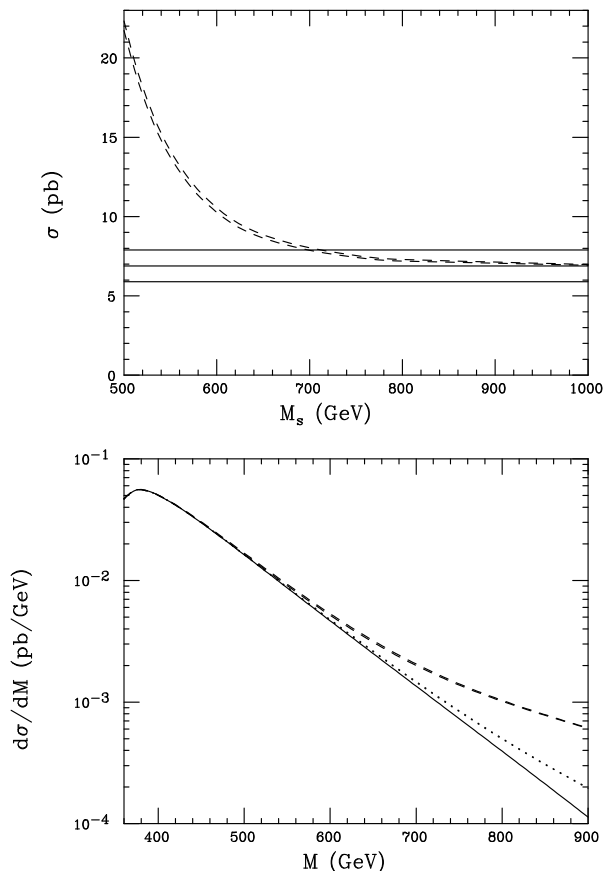


**Figure 9.** Top pair production cross section at Run II of the Tevatron as a function of  $M_s$ . The solid band represents an approximate 15% error on the cross section determination. Although the results for both  $\lambda = \pm 1$  are shown they are visually difficult to separate. Also shown is the top pair invariant mass distribution at Run II of the Tevatron assuming the SM(solid) or  $M_s = 800(1000)$  GeV as the dashed(dotted) curve.

## 5. HERA

$ep$  collisions at HERA allow us to probe  $t$ -channel graviton tower exchange via the processes  $eq, g \rightarrow eq, g$ ; note that the gluon contribution is now present as it was for the Drell-Yan process. By fitting the cross sections at low- $Q^2$  we can extrapolate the cross sections to larger  $Q^2$  to obtain an estimate of the  $M_s$  reach. This result is found to be fairly insensitive to the choice of beam polarization or whether  $e^+$  or  $e^-$  beams are employed. The reach as a function of the integrated luminosity is shown in Fig.11[7].

## 6. $\gamma\gamma$ and $\gamma e$ Colliders

Polarized  $\gamma\gamma$  and  $\gamma e$  collisions may be possible at future  $e^+e^-$  colliders through the use of Compton backscattering of polarized low energy laser beams off of polarized high energy electrons. The resulting backscattered photon distribution,  $f_\gamma(x = E_\gamma/E_e)$ , is far from monoenergetic and is cut off above  $x_{max} \simeq 0.83$  implying that the colliding photons are significantly softer than the parent lepton beam energy. This cutoff at large  $x$  implies that the  $\gamma\gamma(e)$  center of mass energy never exceeds  $\simeq 0.83(0.91)$  of the parent collider. In addition, both the shape of the function  $f_\gamma$  and the average helicity of the produced  $\gamma$ 's are quite sensitive to the polarization state of both the initial laser ( $P_l$ ) and electron ( $P_e$ ) whose values fix the specific distribution.

While it is anticipated that the initial laser polarization will be near 100%, *i.e.*,  $|P_l| = 1$ , the electron beam polarization is expected to be near 90%, *i.e.*,  $|P_e| = 0.9$ . We assume these values in the analysis that follows. With two photon 'beams' and the choices  $P_l = \pm 1$  and  $P_e = \pm 0.9$  to be made for each beam it would appear that 16 distinct polarization-dependent cross sections need to be examined. However, we find that there are only six physically distinct initial polarization combinations. In what follows we will label these possibilities by the corresponding signs of the electron and laser polarizations as  $(P_{e1}, P_{l1}, P_{e2}, P_{l2})$ . (Unpolarized cross sections can be obtained by averaging.) Clearly some of these polarization combinations will be more sensitive to the effects of K-K towers of gravitons than will others.

The first set of processes to examine is  $\gamma\gamma \rightarrow f\bar{f}, gg$  which have so far only fully been examined in the case of unpolarized beams. Note that since there are identical particles in the initial state no  $A_{FB}$  can be formed in this case. The analysis here is similar to that for combined channel  $e^+e^- \rightarrow f\bar{f}$  study in that all accessible final states are included in the fit; the results are shown in Fig.12. The obtainable reach is found to be  $M_s \simeq 4\sqrt{s_{e^+e^-}}$ , somewhat less than in  $e^+e^-$  collisions mostly due to the

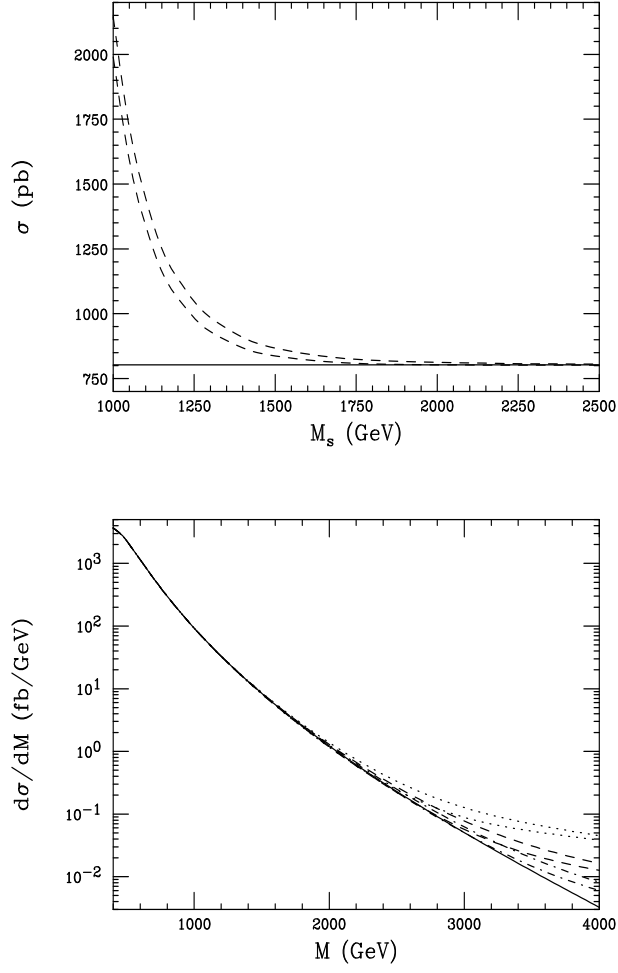


**Figure 10.** Top pair production cross section and pair invariant mass distribution at LHC. In the top quark pair invariant mass plot the values of  $M_s$  were chosen to be 3, 3.5 and 4 TeV with  $\lambda = \pm 1$ .

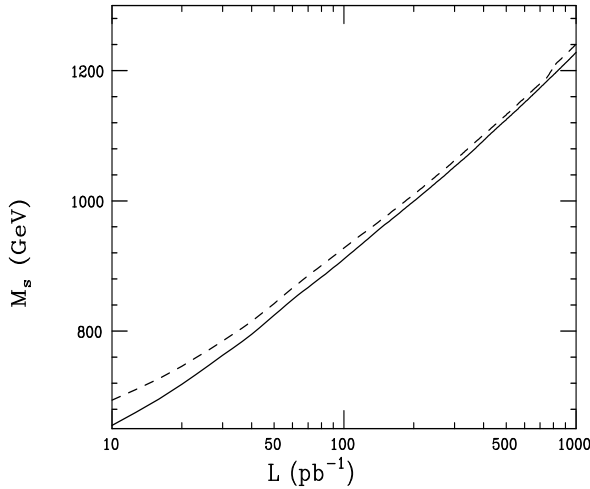


**Figure 11.** 95% CL lower bound on the value of  $M_s$  obtainable at HERA as a function of the integrated luminosity per charge/polarization state for  $\lambda = \pm 1$ .

lower effective center of mass energy of the colliding photons and the lack of polarization information. One would naively expect that the reach for  $M_s$  would increase somewhat if the possibility of beam polarization were included in the analysis.

The  $W^+W^-$  final state offers many observables and very high statistics with which to probe the KK contributions. The differential cross sections are shown in Fig.13 for the SM as well as when the K-K tower is turned for all six initial helicity combinations. Note that in the SM there is no dramatically strong sensitivity to the initial state lepton and laser polarizations and all of the curves have roughly the same shape. When the graviton tower contributions are included there are several effects. First, all of differential distributions become somewhat more shallow at large scattering angles but there is little change in the forward and backward directions due to the dominance of the SM poles. Second, there is now a clear and distinct sensitivity to the initial state polarization selections. In some cases, particularly for the  $(-+-)$  and  $(+--)$  helicity choices, the differential cross section increases significantly for angles near  $90^\circ$  taking on an m-like shape. This shape is, in fact, symptomatic of the spin-2 nature of the K-K graviton tower exchange since a spin-0 exchange leads only to a flattened distribution. Given the very large statistics available with a typical integrated luminosity of  $100 \text{ fb}^{-1}$ , it is clear that the  $\gamma\gamma \rightarrow W^+W^-$  dif-



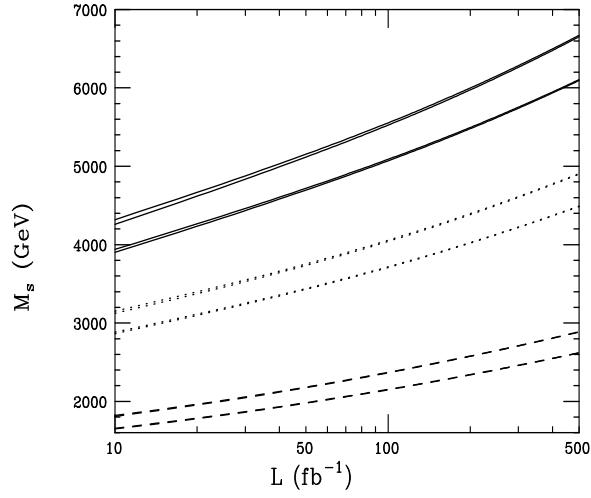


**Figure 12.** Search reaches for the processes  $\gamma\gamma \rightarrow f\bar{f}$ , with  $f$  being the  $c, t$  and  $b$  quarks together with  $e, \mu$  and  $\tau$  (lowest curve of a given type), and for lepton pairs, top, plus light quark jets (upper pair of curves) as a function of the total  $\gamma\gamma$  integrated luminosity. At a 500(1000, 1500) GeV  $e^+e^-$  collider the result is given by the dashed(dotted, solid) curve and in the former case is essentially independent of the choice  $\lambda = \pm 1$ .

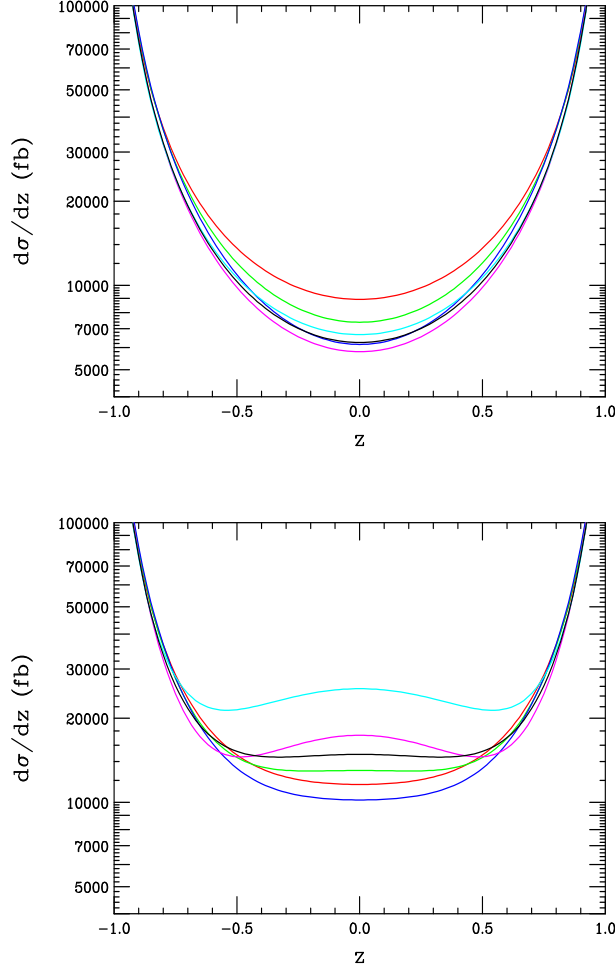


**Figure 13.** Differential cross section for  $\gamma\gamma \rightarrow W^+W^-$  at a 1 TeV  $e^+e^-$  collider for (Top)the SM and with  $M_s = 2.5$  TeV with (Bottom) $\lambda = 1$ . The  $\lambda = -1$  results are nearly identical. In (Top) from top to bottom in the center of the figure the helicities are  $(++++)$ ,  $(+++-)$ ,  $(-++-)$ ,  $(+-++)$ ,  $(+---)$ , and  $(-+-+)$ ; in (Bottom) they are  $(-++-)$ ,  $(+-++)$ ,  $(+++-)$ ,  $(+---)$ ,  $(++++)$ , and  $(-+-+)$

ferential cross section is quite sensitive to  $M_s$  especially for the two initial state helicities specified above.

In the SM, the final state  $W$ 's are dominantly transversely polarized. Due to the nature of the spin-2 graviton exchange, the K-K tower leads to a final state where both  $W$ 's are completely longitudinally polarized. Thus we might expect that a measurement of the  $W$  polarization will probe  $M_s$ . By combining a fit to the total cross sections and angular distributions as well as the  $LL$  and  $LT + TL$  helicity fractions for various initial state polarization choices we are able to discern the discovery as well as the 95% CL exclusion reaches for  $M_s$  as shown in Fig.14. Here we see a reach of  $M - s \sim 11\sqrt{s}$ , which is the larger than that obtained from all other processes examined so far[7].

The process  $\gamma\gamma \rightarrow ZZ$  does not occur at the tree level in the SM or MSSM. This would naively seem to imply that this channel is particularly suitable for looking for new physics effects since the SM and MSSM rates will be so small due to the loop suppression; unfortunately this is not the case. In the case of the ADD scenario the tree level K-K graviton tower contribution is now also present. Neglecting the loop-order SM contributions for the moment we obtain the resulting polarization-dependent differential cross sections shown in Fig.14. The rather small cross section found here leads to a rather poor sensitivity to  $M_s$  of order  $4 - 5\sqrt{s}$ .

## 7. Summary

In this paper we have surveyed some of the processes which can be used to probe for the exchange of KK towers of gravitons in the ADD model. Table I from [13] gives an overall summary of the indirect search reaches for scale  $M_s$ .

## Acknowledgments

The author would like to thank J.L. Hewett for her help in preparing this review.

## References

- [1] N. Arkani-Hamed, S. Dimopoulos and G. Dvali, Phys. Lett. **B429**, 263 (1998) and Phys. Rev. **D59**, 086004 (1999); I. Antoniadis, N. Arkani-Hamed, S. Dimopoulos and G. Dvali, Phys. Lett. **B436**, 257 (1998); N. Arkani-Hamed, S. Dimopoulos and J. March-Russell, hep-th/9809124; P.C. Argyres, S. Dimopoulos and J. March-Russell, Phys. Lett. **B441**, 96

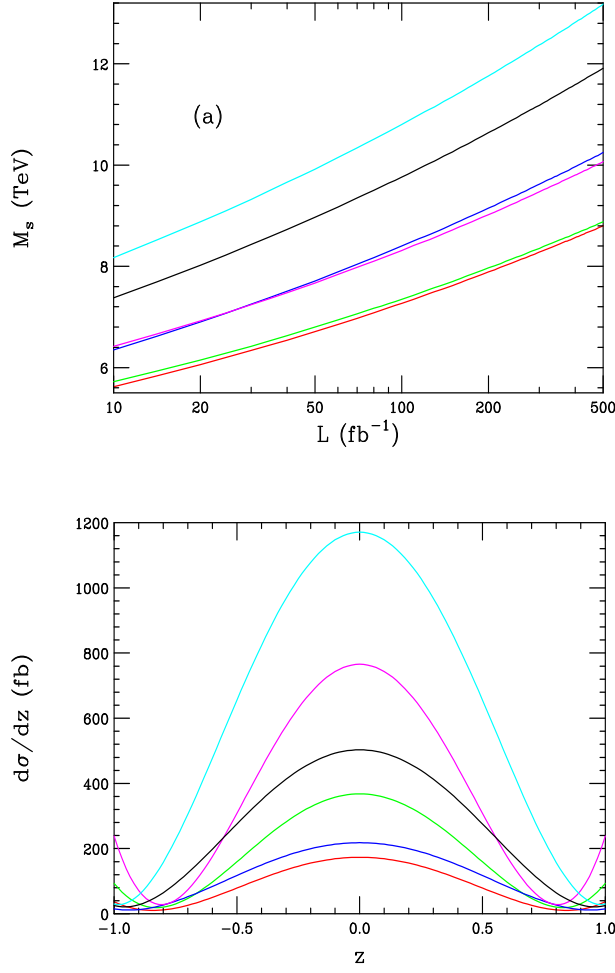


**Figure 14.** (Top)  $M_s$  discovery reach from the process  $\gamma\gamma \rightarrow W^+W^-$  at a 1 TeV  $e^+e^-$  collider as a function of the integrated luminosity for the different initial state polarizations. From top to bottom on the right hand side of the figure the polarizations are  $(- + + -)$ ,  $(+ - - -)$ ,  $(+ + - -)$ ,  $(+ - + -)$ ,  $(+ - - +)$ , and  $(+ + + +)$ . (Bottom) Differential cross section for  $\gamma\gamma \rightarrow ZZ$  at a 1 TeV  $e^+e^-$  collider due to the exchange of a K-K tower of gravitons assuming  $M_s = 3$  TeV. From top to bottom in the center of the figure the initial state helicities are  $(- + + -)$ ,  $(+ - + -)$ ,  $(+ - - -)$ ,  $(+ + + -)$ ,  $(+ + - -)$ ,  $(+ + + +)$ .

Reaction	LEP II ( $2 \text{ fb}^{-1}$ )	LC ( $100 \text{ fb}^{-1}$ )
$e^+e^- \rightarrow ff$	1.15	$6.5\sqrt{s}$
$e^+e^- \rightarrow e^+e^-$	1.0	$6.2\sqrt{s}$
$e^-e^- \rightarrow e^-e^-$		$6.0\sqrt{s}$
$e^+e^- \rightarrow \gamma\gamma$	1.4	$3.2\sqrt{s}$
$e^+e^- \rightarrow WW/ZZ$	0.9	$5.5\sqrt{s}$
	Tevatron ( $2 \text{ fb}^{-1}$ )	LHC ( $100 \text{ fb}^{-1}$ )
$p(\bar{p}) \rightarrow \ell^+\ell^-$	1.4	5.3
$p(\bar{p}) \rightarrow t\bar{t}$	1.0	6.0
$p(\bar{p}) \rightarrow jj$	1.0	
$p(\bar{p}) \rightarrow WW$	0.8	
$p(\bar{p}) \rightarrow \gamma\gamma$	1.4	5.4
	HERA ( $250 \text{ pb}^{-1}$ )	
$ep \rightarrow e + \text{jet}$	1.0	
	$\gamma\gamma$ Collider ( $100 \text{ fb}^{-1}$ )	
$\gamma\gamma \rightarrow \ell^+\ell^-/t\bar{t}/jj$	$4\sqrt{s}$	
$\gamma\gamma \rightarrow \gamma\gamma/ZZ$	$(4-5)\sqrt{s}$	
$\gamma\gamma \rightarrow WW$	$11\sqrt{s}$	

**Table 1.**  $M_s$  search limits in TeV for a number of various processes.

- (1998); Z. Berezhiani and G. Dvali, hep-ph/9811378; N. Arkani-Hamed and S. Dimopoulos, hep-ph/9811353; Z. Kakushadze, hep-th/9811193 and hep-th/9812163; N. Arkani-Hamed *et al.*, hep-ph/9811448; G. Dvali and S.-H.H. Tye, hep-ph/9812483.
- [2] J.C. Long, H.W. Chan and J.C. Price, hep-ph/9805217.
- [3] For an alternative approach to both large and small extra dimensions with asymmetric compactifications, see J. Lykken and S. Nandi, hep-ph/9908505.
- [4] S. Cullen and M. Perelstein, Phys. Rev. Lett. **83**, 268 (1999); L.J. Hall and D. Smith, hep-ph/9904267; V. Barger, T. Han, C. Kao and R.J. Zhang, hep-ph/9905474; G.C. McLaughlin and J.N. Ng, hep-ph/9909558.
- [5] L. Randall and R. Sundrum, hep-ph/9905221 and hep-ph/9906064; W.D. Goldberger and M.B. Wise, hep-ph/9907218 and hep-ph/9907447; H. Davoudiasl, J.L. Hewett and T.G. Rizzo, hep-ph/9909255.
- [6] G.F. Giudice, R. Rattazzi and J.D. Wells, Nucl. Phys. **B544**, 3 (1999); T. Han, J.D. Lykken and R. Zhang, Phys. Rev. **D59**, 105006 (1999), E.A. Mirabelli, M. Perelstein and M.E. Peskin, Phys. Rev. Lett. **82**, 2236 (1999); J.L. Hewett, Phys. Rev. Lett. **82**, 4765 (1999).
- [7] For an incomplete list, see N. Arkani-Hamed, S. Dimopoulos, G. Dvali and J. March-Russell, hep-ph/9811448; N. Arkani-Hamed and S. Dimopoulos, hep-ph/9811353; K. Benakli and S. Davidson, hep-ph/9810280;

Z. Berezhiani and G. Dvali, Phys. Lett. **B450**, 24 (1999), hep-ph/9811378; K.R. Dienes, E. Dudas and T. Gherghetta, hep-ph/9811428; Z. Kakushadze, Nucl. Phys. **B548**, 205 (1999), hep-th/9811193; P. Mathews, S. Raychaudhuri and K. Sridhar, Phys. Lett. **B450**, 343 (1999), hep-ph/9811501; Z. Kakushadze, hep-th/9812163; P. Mathews, S. Raychaudhuri and K. Sridhar, Phys. Lett. **B455**, 115 (1999), hep-ph/9812486; T.G. Rizzo, Phys. Rev. **D59**, 115010 (1999), hep-ph/9901209; A.E. Faraggi and M. Pospelov, Phys. Lett. **B458**, 237 (1999); S.Y. Choi, J.S. Shim, H.S. Song, J. Song and C. Yu, Phys. Rev. **D60**, 013007 (1999), hep-ph/9901368; I. Antoniadis, hep-ph/9904272; M. Dine, hep-ph/9905219; K. Agashe and N.G. Deshpande, Phys. Lett. **B456**, 60 (1999), hep-ph/9902263; T.G. Rizzo, hep-ph/9902273; M.L. Graesser, hep-ph/9902310; Z. Silagadze, hep-ph/9907328 and hep-ph/9908208; Z. Kakushadze, Nucl. Phys. **B551**, 549 (1999), hep-th/9902080; T. Banks, M. Dine and A. Nelson, JHEP **06**, 014 (1999), hep-th/9903019; K. Cheung and W. Keung, hep-ph/9903294; S. Cullen and M. Perelstein, Phys. Rev. Lett. **83**, 268 (1999); T.G. Rizzo, Phys. Rev. **D60**, 075001 (1999); D. Atwood, S. Bar-Shalom and A. Soni, hep-ph/9903538; C. Balazs, H. He, W.W. Repko, C.P. Yuan and D.A. Dicus, hep-ph/9904220; P. Mathews, S. Raychaudhuri and K. Sridhar, hep-ph/9904232; A.K. Gupta, N.K. Mondal and S. Raychaudhuri, hep-ph/9904234; G. Shiu, R. Shrock and S.H. Tye, Phys. Lett. **B458**, 274 (1999); K. Cheung, hep-ph/9904266; L.J. Hall and D. Smith, hep-ph/9904267; H. Goldberg, hep-ph/9904318; K.Y. Lee, H.S. Song and J. Song, hep-ph/9904355; T.G. Rizzo, hep-ph/9904380; H. Davoudiasl, hep-ph/9904425; K. Yoshioka, hep-ph/9904433; K. Cheung, Phys. Lett. **B460**, 383 (1999); K.Y. Lee, H.S. Song, J. Song and C. Yu, hep-ph/9905227; X. He, hep-ph/9905295; P. Mathews, P. Poulose and K. Sridhar, hep-ph/9905395; T. Han, D. Rainwater and D. Zeppenfeld, hep-ph/9905423; V. Barger, T. Han, C. Kao and R.J. Zhang, hep-ph/9905474; X. He, hep-ph/9905500; A. Pilaftsis, hep-ph/9906265; D. Atwood, S. Bar-Shalom and A. Soni, hep-ph/9906400; H. Davoudiasl, hep-ph/9907347; D. Bourilkov, hep-ph/9907380, T.G. Rizzo hep-ph/9907401; R.N. Mohapatra, S. Nandi and A. Perez-Lorenzana, hep-ph/9907520; A. Ioannisian and A. Pilaftsis, hep-ph/9907522; P. Das and S. Raychaudhuri, hep-ph/9908205; H.-C. Cheng and K.T. Matchev, hep-ph/9908328; O.J.P. Eboli, T. Han, M.B. Margo and P.G. Mercadante, hep-ph/9908538; X.-G. He, G.C. Joshi and B.H.J. McKellar, hep-ph/9908469; J. Lykken and S. Nandi, hep-ph/9908505; S. Chang, S. Tazawa and M. Yamaguchi, hep-ph/9908515; K. Cheung and G. Landsberg, hep-ph/9909218; D.K. Ghosh, P. Poulose and K. Sridhar, hep-ph/9909377; D. Atwood, S. Bar-Shalom and A. Soni, hep-ph/9909392; D.K. Ghosh *et al.*, hep-ph/9909567.

- [8] See, for example, ALEPH Collaboration, ALEPH note 99-051; DELPHI Collaboration, DELPHI notes 99-135 and 99-137; L3 Collaboration, hep-ex/9909019 and L3 note 2418 (1999); OPAL Collaboration, hep-ex/9907064 and CERN-EP/99-097. See also D. Bourilkov, hep-

- ph/9907380 and S. Mele and E. Sanchez, hep-ph/9909294.
- [9] I. Antoniadis, K. Benalki and M. Quiros, hep-ph/9905311; M. Bando, T. Kugo, T. Noguchi and K. Yoshioka, hep-ph/9906549; J. Hisano and N. Okada, hep-ph/9909555.
  - [10] N. Arkani-Hamed and M. Schmaltz, hep-ph/9903417; N. Arkani-Hamed, Y. Grossman and M. Schmaltz, hep-ph/9909411.
  - [11] T.G. Rizzo, Phys. Rev. **D59**, 113004 (1999).
  - [12] For a review, see J.L. Hewett and T.G. Rizzo, Phys. Rev. **D56**, 5709 (1997) and Phys. Rev. **D58**, 055005 (1998).
  - [13] J.L. Hewett, talk given at the *World-Wide Study of Physics and Detectors for Future Linear Colliders(LCWS99)*, Sitges, Barcelona, Spain, 28 April-5 May 1999.